Journal of Veterinary Cardiology (2019) **21**, 79—92

ELSEVIER

Journal of Veterinary Cardiology
ESVC

www.elsevier.com/locate/jvc

# Quantitative assessment of two- and three-dimensional transthoracic and two-dimensional transesophageal echocardiography, computed tomography, and magnetic resonance imaging in normal canine hearts

**R.C. Fries, DVM [a,*], S.G. Gordon, DVM [a], A.B. Saunders, DVM [a], M.W. Miller, DVM [a], C.D. Hariu, DVM [a], D.J. Schaeffer, Ph.D [b]**

[a] *Texas A&M University College of Veterinary Medicine and Biomedical Sciences, 4474 TAMU, College Station, TX 77843-4474, USA*
[b] *University of Illinois College of Veterinary Medicine, 1008 West Hazelwood Drive, Urbana, IL 61802, USA*

Received 18 May 2018; received in revised form 8 September 2018; accepted 20 September 2018

**KEYWORDS**
Cardiac;
Comparison;
Ejection fraction;
Reproducibility;
Variability

**Abstract** *Introduction:* The objective of the study was to evaluate the accuracy of two- and three-dimensional (2D, 3D) transthoracic echocardiography (TTE), 2D transesophageal echocardiography, and computed tomography angiography (CTA) compared with cardiac magnetic resonance imaging (CMR) in normal dogs and to assess repeatability of 2D and 3D TTE for the assessment of left ventricular (LV) and left atrial (LA) dimensions.
*Animals:* The study was performed on six healthy dogs.
*Materials and Methods:* Transthoracic echocardiography, transesophageal echocardiography, CTA, and CMR were performed on each dog. Right ventricular (RV) and LV volumes (in systole and diastole), ejection fraction (EF), and LA and right atrial (RA) volumes were assessed. Repeatability and intrarater and interrater measurements of variability were quantified by average coefficient of variation (CV) for 2D and 3D TTE.
*Results:* No clinically relevant differences in LV volume were detected between CMR and all modalities. Importantly, 3D TTE had the lowest CV (6.45%), correlated with ($r_s = 0.62$, $p = 0.01$), and had the highest overlap in distribution with CMR (OVL

* Corresponding author.
*E-mail address:* rfries@illinois.edu (R.C. Fries).

https://doi.org/10.1016/j.jvc.2018.09.005

>80%). Left ventricular EF and LA size via CTA compared best with CMR and RV and RA volumes were best estimated by 3D TTE. Assessment of LV and LA volumes via 3D TTE had moderate repeatability (15—21%) compared with LV M-mode measurements and 2D LA-to-aortic ratio (<10%), respectively. For LV size, interrater CV for 3D TTE (19.4%) was lower than 2D TTE (23.1%).
*Conclusions:* Measurements of LV, RV, and RA volumes via 3D TTE and LA volume and LV EF assessed by CTA compared best with CMR. Three-dimensional echocardiography had lower interrater and intrarater CV compared with 2D TTE.


**Abbreviations**

| | |
|---|---|
| 2D | two-dimensional |
| 3D | three-dimensional |
| CI | confidence interval |
| CMR | cardiac magnetic resonance imaging |
| CTA | computed tomography angiography |
| CV | coefficient of variation |
| EDV (mL) | end-diastolic volume |
| ESV (mL) | end-systolic volume |
| EF (%) | ejection fraction |
| IV | intravenous |
| L-4CH | left apical four-chamber view |
| LA | left atrium |
| LA:Ao | left atrium-to-aortic root ratio |
| LV | left ventricle |
| OVL (%) | overlapping distribution |
| R-4CH | right parasternal four-chamber view |
| RA | right atrium |
| RV | right ventricle |
| SMOD | Simpson's method of discs |
| TEE | transesophageal echocardiography |
| TTE | transthoracic echocardiography |

## Introduction

Transthoracic echocardiography (TTE) is the standard for non-invasive assessment of cardiac function, anatomy, and pathology. Standard imaging planes have been described for two-dimensional (2D) TTE and transesophageal echocardiography (TEE) in dogs [1,2]. However, availability of newer modalities such as real-time three-dimensional (3D) echocardiography, computed tomography angiography (CTA), and cardiac magnetic resonance imaging (CMR) warrants their validation in normal canine hearts.

Accuracy of left ventricular (LV) volume and ejection fraction (EF) derived from 2D TTE and 2D TEE images is limited by image orientation, geometric assumptions, and boundary tracing errors [3]. Real-time 3D TTE, CTA, and CMR avoid geometric assumptions and modeling, and CTA and CMR can acquire images in any orientation [4,5]. Transthoracic 3D echocardiography also avoids geometric assumption; however, it is constrained to standard imaging windows. Cardiac magnetic resonance imaging is considered the non-invasive reference standard for cardiac function and mass in humans and the preferred imaging modality when precise quantification is vital [6,7]. Several human studies have validated 3D TTE for anatomical and functional assessment of the heart [8—10]. Few studies have attempted validation of 3D TTE or CTA for canine hearts [11—13]. These studies reported notable correlations between 3D TTE and LV mass and volume on excised canine hearts or were validated using antiquated 3D technology [14,15]. Furthermore, the role of 3D TTE in human cardiology has expanded to include comprehensive assessment of the right heart [16—19].

Owing to limitations of 2D TTE in accurately assessing heart anatomy and function, improved non-invasive imaging modalities are desirable. Modalities such as 3D TTE and CTA are promising great potential for assessing human cardiac anatomy and function [20—22]. Agreement with a reference standard is an essential component for assessment of any modality; however, the ability to consistently replicate images as a single observer, and between observers, is vital for clinical application, particularly for individual longitudinal patient monitoring and design and analysis of clinical studies. Given the limited availability and need for general anesthesia for TEE, CTA, and CMR, we sought to determine the variability of 2D TTE and 3D TTE for commonly assessed cardiac parameters and determine the optimal number of repetitions required per modality when assessing these parameters. We hypothesized that 3D TTE, 2D TEE, and CTA would compare more closely with a CMR reference standard than 2D TTE and 2D TTE would be more repeatable than 3D TTE.

## Animals, materials, and methods

This study was approved by the Institutional Animal Care and Use Committee and the Clinical Research Review Committee at Texas A&M University.

### Animals

Six, adult, female mixed breed dogs (18—25 kg), from an X-linked nephropathy research colony at Texas A&M University College of Veterinary Medicine and Biomedical Sciences, were used. Dogs were heterozygous carriers for the genetic disorder affecting glomerular basement membrane collagen, which cardiac involvement is not reported [23—26]. Enrolled dogs were considered to have healthy normal hearts based on history, physical examination, thoracic radiographs, 2D TTE, Doppler systemic blood pressure, biochemistry panel, complete blood count, and urinalysis.

### Modality comparison

Dogs were anesthetized using a standardized protocol: butorphanol 0.2 mg/kg intravenous (IV), midazolam 0.1 mg/kg IV, propofol 3 mg/kg IV, and isoflurane (end-tidal volume of 1.5% in oxygen). Each study was performed sequentially: 2D TTE, 3D TTE, 2D TEE, CTA, and CMR. Hemodynamic variables, heart rate, blood pressure, and depth of anesthesia were maintained in a narrow range throughout: average heart rate, 90—110 beats/min; ventilator respiratory rate maintained at 8—11 breaths/min and exhaled PCO2 between 25 and 40 mmHg; and mean arterial blood pressure between 80 and 100 mmHg. As needed, glycopyrrolate (0.005—0.01 mg/kg IV) was administered to maintain heart rate.

Echocardiographic examinations were performed by a single investigator (R.C.F.) using an ultrasonographic scanner[c] equipped with a phased-array 5 MHz transducer, a matrix-array 3-V transducer, a 6T TEE transducer, and simultaneous electrocardiogram monitoring. Dogs were positioned in right and left lateral recumbency on a raised table for dependent imaging and in right lateral for TEE. Images and loops were digitally stored and sent to a workstation equipped with software[d] for off-line analysis. Echocardiographic methods were analyzed by the same investigator (R.C.F.) in a random order, blinded to patient information and study number. Measurements were repeated from five different cardiac cycles obtained during the same anesthetic session, and mean values were used for statistical analysis.

### Two-dimensional transthoracic echocardiography

All dogs underwent complete TTE that included 2D, M-mode, spectral, and color flow Doppler. Images were obtained in accordance with techniques and imaging planes described elsewhere [1]. To assess individual chamber sizes, images were optimized to include the apex of both ventricles in the right parasternal long-axis four-chamber view (R-4CH) and left apical 4-chamber view (L-4CH), ensuring maximal length of both ventricles. Both atria were optimized in the L-4CH, ensuring interatrial and free-wall endocardial surfaces were visualized. Separate images were saved if atria or ventricles could not be optimized simultaneously.

#### Left ventricular M-mode and left atrium 2D

M-mode images were acquired from 2D TTE as previously described and included LV internal dimension in diastole and systole [1]. The left atrium (LA) to aortic root ratio (LA:Ao) was measured from 2D and M-mode images as previously described [1,27].

#### Left ventricular volume

Monoplane Simpson's method of discs (SMOD) measurements of the LV were performed from the R-4CH and L-4CH as previously described [28]. Manual tracing of the endocardial border in diastole and systole was performed. Papillary muscles and trabeculae were not traced around and, therefore, included in LV volume calculation. Volumes and EF were automatically calculated by use of the summation of 15 elliptical disks utilizing the EchoPAC[d] system software.

#### Left atrial volume

The LA maximum volume was calculated using the modified monoplane SMOD from the L-4CH, defined as the volume after end LV systole immediately before mitral valve opening (end of isovolumetric relaxation). The LA endocardial border was traced, and volume was calculated by EchoPAC[d] software (Fig. 1). The pulmonary vein confluences and LA appendage were excluded.

[c] Vivid E9, GE Medical System, Waukesha, WI, USA.
[d] EchoPac, version BT09, GE Medical System, Waukesha, WI, USA.

### Right ventricular volume

Monoplane SMOD measurements of the right ventricle (RV) were performed from the R-4CH and modified L-4CH as previously described [29,30]. Manual tracing of the endocardial border in diastole and systole was performed. Papillary muscles and trabeculae were not traced around and, therefore, included in the RV volume calculation. Volumes and EF were automatically calculated utilizing the EchoPAC[d] system.

### Right atrial volume

The right atrial (RA) maximum volume was calculated using the monoplane SMOD from the L-4CH and was defined as the volume after end RV systole immediately before tricuspid valve opening (end of isovolumetric relaxation). The RA endocardial border was traced, and a straight line was drawn between the attachment points of the tricuspid annulus. Volume was calculated automatically by the EchoPAC[d] software (Fig. 2).

## Three-dimensional transthoracic echocardiography

All dogs underwent a complete 3D TTE obtaining the same images as 2D TTE. Full volume loops of all cardiac chambers were created using a 3V matrix-array transducer obtaining pyramidal volumes in real time over three sequential cardiac cycles with a frame rate >12 frames per second. The entire cardiac chamber was displayed simultaneously using a quad screen layout. Measurements were performed off-line using four-dimensional semi-automatic border detection software.[d] Manual corrections were performed in cases of egregiously inaccurate endocardial automated detection.

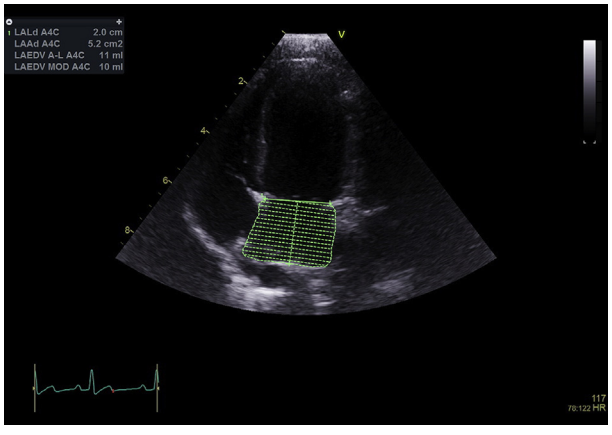


**Fig. 1** Representative snapshot of the workstation output for left atrial volume determined from the left apical four-chamber view.

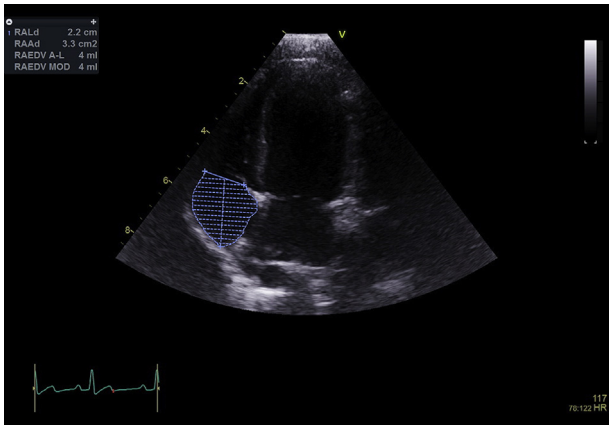


**Fig. 2** Representative snapshot of the workstation output for right atrial volume determined from the left apical four-chamber view.

Minor errors were allowed so integrity and accuracy of the software could be determined.

### Three-dimensional left and right ventricular volumes

Ventricular volumes were measured from the L-4CH, optimized for either the LV or RV, as described in the preceding Two-dimensional transthoracic echocardiography section. The software requires identification of end-diastolic and end-systolic frames and three anatomic landmarks. The LV landmarks included anterior and posterior mitral annulus and LV apex. The RV landmarks included septal and posterior borders of the tricuspid valve and RV apex. Semiautomated border detection was performed by the software, and ventricular endocardial borders were tracked throughout the entire cardiac cycle. Software computed LV and RV end-diastolic volume (EDV), end-systolic volume (ESV), and EF by use of a geometric algorithm that relies on computer artificial intelligence and pattern recognition, creating a dynamic cast of the ventricular cavities. The computer algorithm assumes that when the ultrasound is parallel with the ventricular walls, in the apical views, the apex and insertion points of the valves are the strongest reflector points and represent key reference points for automated cardiac silhouette delineation [31].

### Three-dimensional left and right atrial volumes

Atrial volumes were measured from the L-4CH view at end-systole, optimized for either atria, as described in the preceding Two-dimensional transthoracic echocardiography section. The volume software requires the investigator to identify both an end-diastolic and end-systolic frame to utilize the software. An end-diastolic frame was

selected and measured but not recorded. The three anatomic landmarks used for the RA included septal and posterior borders of the tricuspid valve and dorsal border of the RA. Landmarks for the LA included anterior and posterior borders of the mitral valve and dorsal border of the LA. Semiautomated border detection was performed by the software. Software computed LA and RA EDV, ESV, and EF by use of a geometric algorithm and created a dynamic cast of the atria.

## Two-dimensional transesophageal echocardiography

The transducer was advanced aborally down the esophagus into the transgastric position and then pulled back orally until images of the LV were obtained from the middle position [2]. A transverse plane of the middle position allowed acquisition of a longitudinal 4CH of the LV. Images were optimized for maximum LV chamber size, endocardial detail, and visualization of the apex. Measurements were performed from this view.

### Left ventricular volume TEE

Monoplane SMOD was used to measure LV volume. End-diastolic and end-systolic frame selection and measurements were carried out as outlined in the preceding Two-dimensional transthoracic echocardiography section.

## Computed tomography angiography

Computed tomography angiography images were obtained with a Siemens Biograph mCT 128-slice PET scanner.[e] Radiograph scout views were performed for positioning and planning using fully assisted scanner software. A test IV bolus of 3 mL non-iodinating contrast agent (Iohexol[f]) was injected into the cephalic vein to determine optimal timing for imaging of the LA and LV. Gated cardiac CTA was performed beginning with a 10 mL injection of contrast in the cephalic vein followed by image acquisition trigged to the appearance of contrast in the RV, allowing for sufficiency delay and maximum contrast in the LV and LA. Imaging parameters included 3000-msec gantry rotation speed, 0.33 mm isotropic resolution, and a voltage of 120 kV with a current of 117 mA. Scan data were reconstructed at 0.6-mm slice thickness with 150 msec temporal resolution. Images were acquired during breath holding at end-expiration by turning the respirator off (average, 8 s), and data were digitally stored for off-line analysis. All CTA images were analyzed using a Siemens workstation and associated software.[g] Measurements from this data set of averaged cardiac cycles were measured 3 times, and mean values were used for statistical analysis.

### Left ventricular volume CTA

The LV endocardial boundary was traced semiautomatically and manually adjusted when necessary. Papillary muscles and trabeculae were traced around and, therefore, excluded from LV volume calculation. The software calculated EDV, ESV, and EF by use of SMOD equation.

### Left atrial volume CTA

The LA end-systolic phase was defined as the largest LA before mitral valve opening. Oblique multiplanar reformation was performed to obtain two- and four-chamber views, which were reconstructed along the LA long axis. Endocardial borders were manually traced, and the LA appendage was included, while the pulmonary veins were excluded from analysis.

### Right ventricular volume CTA

This was not performed because of the lack of contrast.

### Right atrial volume CTA

This was not performed because of the lack of contrast.

## Cardiac magnetic resonance imaging

The CMR images were obtained with a 32-channel whole-body 3T system[h] with phased-array cardiac coils. Gated Flash cine mode was used to acquire dynamic loops of the heart and stacks of short-axis images from the aortic root to apex with the following parameters: 5-mm slice thickness with no gaps, 300 mm field of view, read matrix = 192, phase matrix = 128, resulting mean pixel size = 2.2 × 1.9 mm, 50.4 ms repetition time, 2.4 ms echo time, and a 44° pulse flip angle. Images were acquired during breath holding at end-expiration by turning the respirator off

[e] SOMATOM Definition AS+, Siemens Medical Solutions, Malvern, PA, USA.

[f] Omnipaque 300TM Iohexol injection, GE Healthcare, Princeton, NJ, USA.

[g] Syngo-X Workplace, Siemens Medical Solutions, Malvern, PA, USA.

[h] MAGNETOM Verio; Siemens AG, Healthcare Sector Erlangen, Germany.

(average, 12 s) and stored digitally for off-line analysis. Volumes were calculated using Siemens Argus[i] software. Measurements from this data set of averaged cardiac cycles were measured 3 times, and mean values were used for statistical analysis.

**Left ventricular volume CMR**
Volume was assessed from the first basal slice showing 50% circumference of the LV cavity surrounded by myocardial tissue through the last apical slice of LV cavity. Endocardial boundary was manually traced in every slice at end-diastole (defined visually as the largest LV cavity) and end-systole (defined visually as the smallest LV cavity), with papillary muscles and trabeculae traced around, and, therefore, excluded from the LV cavity. The software calculated EDV, ESV, and EF by use of SMOD equation.

**Left atrial volume CMR**
Volume was measured by a standard short-axis method, where maximal LA volume was defined as end ventricular systole immediately before mitral valve opening. Manual tracing of endocardial borders of successive slices was performed from the dorsal wall of the LA to the atrioventricular junction. The LA appendage was included in LA volume, whereas pulmonary veins were excluded. The maximum LA volume was calculated from the sums of outlined areas using a modification of SMOD.

**Right ventricular volume CMR**
Volume was measured in the short-axis plane and involved manual tracing of endocardial contours for each short-axis slice at end-systole and end-diastole from base to apex. The RV base was defined as the portion of RV (including outflow) below the tricuspid valve annulus (Fig. 3). Papillary muscles and trabeculae were traced around and, therefore, excluded from the RV volume calculation. The software calculated EDV, ESV, and EF by use of SMOD equation.

**Right atrial volume CMR**
Volume was measured by a short-axis method, where maximal RA volume was defined as end-systole immediately before tricuspid valve opening. Manual tracing of endocardial borders of successive slices was performed from the dorsal wall of the RA to the atrioventricular junction. The RA appendage was included in the RA volume, whereas the caudal and cranial vena cava were excluded. The maximal RA volume was calculated from sums of the outlined areas using a modification of SMOD.

[i] Argus, Siemens AG, Healthcare Sector Erlangen, Germany.

## Variability

Five, conscious, unsedated dogs underwent complete 2D TTE and 3D TTE examinations by four investigators. Each dog had five complete studies performed by each investigator over 2—7 days. The right and left parasternal views of the LV and LA were obtained and measured as described in the preceding Two-dimensional transthoracic echocardiography, Three-dimensional transthoracic echocardiography, and M-mode sections. Examiners obtained and measured only their own images either on the echocardiographic machine used to acquire the images or an EchoPac[d] workstation.

One additional investigator obtained five complete 2D TTE and 3D TTE studies on one dog over 2 days. Three different investigators (R.C.F., S.G.G., A.B.S.), blinded to each other's results, performed measurements on these studies.

## Statistical analysis

Three data sets were obtained to quantify agreement and variability of the imaging modalities. All data sets were used to examine at least two questions. Each question used several statistical

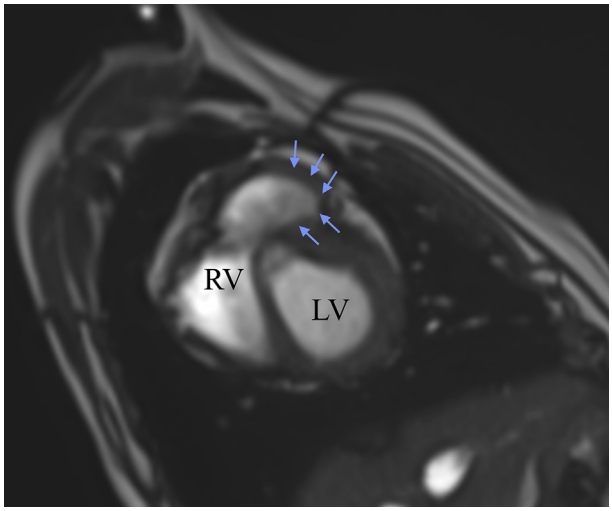


**Fig. 3** Representative cardiac magnetic resonance (CMR) image of the right ventricle and right ventricular outflow tract from the short-axis plane at the level of the heart base, apical to the tricuspid valve. The right ventricular outflow tract is outlined by the blue arrows. LV, left ventricle; RV, right ventricle.

**Table 1** Descriptive statistics for echocardiographic, computed tomographic, and magnetic resonance imaging parameters in six adult mixed breed dogs.

| Six adult mixed breed dogs, mean body weight = 25.2 kg (min = 21.9; max = 28.9) | | | | | | | |
|---|---|---|---|---|---|---|---|
| Variable | Unit | N | Mean | Standard deviation | Median | Min | Max |
| LVEDV_CMR | mL | 18 | 48.50 | 5.980 | 50.00 | 41.00 | 54.00 |
| LVEDV_3D | mL | 30 | 45.37 | 5.666 | 46.00 | 34.00 | 53.00 |
| LVEDV_R-4CH | mL | 30 | 46.50 | 3.893 | 46.50 | 39.00 | 54.00 |
| LVEDV_L-4CH | mL | 30 | 46.73 | 6.051 | 46.00 | 35.00 | 57.00 |
| LVEDV_CT | mL | 18 | 48.67 | 5.980 | 49.50 | 38.00 | 60.00 |
| LVEDV_TEE | mL | 30 | 49.23 | 5.770 | 50.50 | 38.00 | 62.00 |
| LVESV_CMR | mL | 18 | 21.56 | 2.791 | 21.00 | 18.00 | 28.00 |
| LVESV_3D | mL | 30 | 22.10 | 3.055 | 22.00 | 16.00 | 28.00 |
| LVESV_R-4CH | mL | 30 | 21.30 | 2.493 | 22.00 | 17.00 | 25.00 |
| LVESV_L-4CH | mL | 30 | 21.80 | 3.188 | 22.00 | 14.00 | 29.00 |
| LVESV_CT | mL | 18 | 22.50 | 2.936 | 22.50 | 17.00 | 27.00 |
| LVESV_TEE | mL | 30 | 21.87 | 3.550 | 21.50 | 16.00 | 29.00 |
| LV_EF_CMR | % | 18 | 55.38 | 5.478 | 54.61 | 48.00 | 66.04 |
| LV_EF_3D | % | 30 | 51.09 | 5.430 | 51.86 | 39.02 | 58.97 |
| LV_EF_R-4CH | % | 30 | 54.09 | 4.970 | 54.26 | 44.44 | 61.70 |
| LV_EF_L-4CH | % | 30 | 53.22 | 4.922 | 53.52 | 44.44 | 62.26 |
| LV_EF_CT | % | 30 | 53.51 | 5.456 | 53.49 | 43.18 | 65.31 |
| LV_EF_TEE | % | 30 | 55.57 | 5.147 | 56.5 | 46.94 | 65.38 |
| LA_CMR | mm | 18 | 21.78 | 1.833 | 22.00 | 18.00 | 25.00 |
| LA_3D | mm | 30 | 19.57 | 3.390 | 18.50 | 14.00 | 26.00 |
| LA_CT | mm | 18 | 22.56 | 2.202 | 22.00 | 19.00 | 28.00 |
| LA_2D | mm | 30 | 23.97 | 5.147 | 24.00 | 18.00 | 32.00 |
| RVEDV_CMR | mL | 18 | 29.33 | 6.324 | 26.50 | 21.00 | 39.00 |
| RVEDV_3D | mL | 30 | 20.83 | 5.187 | 21.50 | 13.00 | 30.00 |
| RVEDV_R-4CH | mL | 30 | 12.13 | 2.300 | 12.00 | 8.00 | 16.00 |
| RVEDV_L-4CH | mL | 30 | 12.20 | 3.210 | 12.00 | 7.00 | 19.00 |
| RVESV_CMR | mL | 18 | 13.94 | 2.754 | 14.00 | 9.00 | 18.00 |
| RVESV_3D | mL | 30 | 11.33 | 3.315 | 11.00 | 7.00 | 19.00 |
| RVESV_R-4CH | mL | 30 | 6.20 | 1.495 | 6.00 | 4.00 | 10.00 |
| RVESV_L-4CH | mL | 30 | 5.50 | 1.456 | 5.00 | 3.00 | 8.00 |
| RV_EF_CMR | % | 18 | 51.95 | 6.983 | 54.30 | 37.04 | 59.09 |
| RV_EF_3D | % | 30 | 44.98 | 10.748 | 46.55 | 25.00 | 60.00 |
| RV_EF_R-4CH | % | 30 | 48.12 | 12.740 | 50.00 | 35.71 | 66.67 |
| RV_EF_L-4CH | % | 30 | 53.27 | 13.165 | 56.35 | 22.22 | 70.59 |
| RA_CMR | mm | 18 | 21.56 | 3.203 | 20.00 | 17.00 | 29.00 |
| RA_3D | mm | 30 | 18.00 | 5.058 | 17.00 | 11.00 | 29.00 |
| RA_2D | mm | 30 | 13.23 | 3.287 | 13.50 | 8.00 | 18.00 |

3D, three-dimensional; AP, apical four-chamber; CMR, cardiac magnetic resonance imaging; CT, computed tomography; L-4CH, left apical four-chamber; LA, left atrium; LVEDV, left ventricular end-diastolic volume; LV_EF, left ventricular ejection fraction; LVESV, left ventricular end-systolic volume; R-4CH, right parasternal four-chamber; RA, right atrium; RVEDV, right ventricular end-diastolic volume; RV_EF, right ventricular ejection fraction; RVESV, right ventricular end-systolic volume; TEE, transesophageal.

analyses. Questions, data, and primary analyses are summarized in Table 5.

Summary statistics (N, mean, median, standard deviation, skew, kurtosis, and Shapiro—Wilk and Anderson—Darling tests of normality) were calculated for all data sets by investigator, modality, and dog. Where appropriate, summary statistics were also calculated for all investigators by modality, for all dogs by investigator and modality, and all dogs by modality for all investigators. Time entered as repeated measures for multiple imaging sessions for an investigator and modality and for multiple measurement sessions for each investigator and modality. Investigators chose their own times for acquiring and measuring images and the order in which images from different modalities were evaluated, and such random ordering was not considered.

**Table 2** Comparison between magnetic resonance imaging and echocardiographic and computed tomographic variables in healthy dogs.

| Parameter | Method | Mean | Unit | IQR | 95% Confidence limits | | OVL | CV | R_Spearman | *p* |
|---|---|---|---|---|---|---|---|---|---|---|
| LVEDV | 3D | −3.13 | mL | 10.00 | −6.29 | 0.02 | 0.8048 | 6.20% | 0.61 | 0.01 |
| LVEDV | R-4CH | −2.00 | mL | 5.00 | −5.16 | 1.16 | 0.7804 | 7.10% | 0.47 | 0.05 |
| LVEDV | L-4CH | −1.77 | mL | 7.00 | −4.92 | 1.39 | 0.8106 | 5.30% | 0.00$^{+++}$ | 0.10 |
| LVEDV | CT | 0.17 | mL | 6.00 | −3.36 | 3.70 | 0.8384 | 8.10% | 0.00$^{+++}$ | 0.85 |
| LVEDV | TEE | 0.73 | mL | 9.00 | −2.42 | 3.89 | 0.8654 | 7.80% | 0.44 | 0.07 |
| LVESV | 3D | 0.54 | mL | 4.00 | −2.61 | 3.70 | 0.8273 | 6.70% | 0.63 | 0.01 |
| LVESV | R-4CH | −0.26 | mL | 4.00 | −3.41 | 2.90 | 0.8465 | 8.90% | 0.00$^{+++}$ | 0.30 |
| LVESV | L-4CH | 0.24 | mL | 4.00 | −2.91 | 3.40 | 0.8117 | 9.00% | 0.53 | 0.02 |
| LVESV | CT | 0.94 | mL | 4.00 | −2.59 | 4.47 | 0.8121 | 10.40% | 0.55 | 0.02 |
| LVESV | TEE | 0.31 | mL | 6.00 | −2.85 | 3.47 | 0.8319 | 12.20% | 0.00$^{+++}$ | 0.36 |
| LV_EF | 3D | −4.30 | % | 7.59 | −7.45 | −1.14*** | 0.7782 | 8.80% | 0.67 | 0.01 |
| LV_EF | R-4CH | −1.29 | % | 8.20 | −4.45 | 1.86 | 0.9124 | 8.40% | 0.00$^{+++}$ | 0.74 |
| LV_EF | L-4CH | −2.16 | % | 8.84 | −5.40 | 1.66 | 0.8622 | 7.50% | 0.00$^{+++}$ | 0.68 |
| LV_EF | CT | −1.87 | % | 6.86 | −5.32 | 1.00 | 0.8827 | 9.00% | 0.61 | 0.01 |
| LV_EF | TEE | 0.18 | % | 6.57 | −2.97 | 3.34 | 0.9238 | 9.40% | 0.00$^{+++}$ | 0.06 |
| LA | 2D | 2.19 | mL | 4.00 | −0.97 | 5.35 | 0.6364 | 10.00% | 0.00$^{+++}$ | 0.31 |
| LA | 3D | −2.21 | mL | 5.00 | −5.37 | 0.95 | 0.5689 | 7.20% | 0.00$^{+++}$ | 0.34 |
| LA | CT | 0.78 | mL | 2.00 | −2.75 | 4.31 | 0.8955 | 8.70% | 0.00$^{+++}$ | 0.68 |
| RVEDV | 3D | −8.5 | mL | 10.00 | −11.66 | −5.34*** | 0.5793 | 11.40% | 0.86 | 0.01 |
| RVEDV | R-4CH | −17.2 | mL | 3.00 | −20.36 | −14.0*** | 0.0424 | 14.70% | 0.00$^{+++}$ | 0.68 |
| RVEDV | L-4CH | −17.13 | mL | 5.00 | −20.29 | −13.9*** | 0.1002 | 14.90% | 0.00$^{+++}$ | 0.09 |
| RVESV | 3D | −2.61 | mL | 4.00 | −5.77 | 0.55 | 0.6511 | 15.10% | 0.66 | 0.01 |
| RVESV | R-4CH | −7.74 | mL | 2.00 | −10.90 | −4.59*** | 0.1321 | 20.20% | 0.12 | 0.63 |
| RVESV | L-4CH | −8.44 | mL | 3.00 | −11.60 | −5.29*** | 0.0863 | 17.30% | 0.30 | 0.22 |
| RV_EF | 3D | −6.97 | % | 19.17 | −10.12 | −3.81*** | 0.7093 | 23.60% | 0.46 | 0.06 |
| RV_EF | R-4CH | −3.83 | % | 16.25 | −6.99 | −0.67*** | 0.7706 | 24.90% | 0.00$^{+++}$ | 0.20 |
| RV_EF | L-4CH | 1.33 | % | 18.72 | −1.83 | 4.48 | 0.6560 | 21.20% | 0.00$^{+++}$ | 0.57 |
| RA | 2D | −8.32 | mL | 6.00 | −11.48 | −5.17*** | 0.2407 | 11.90% | 0.00$^{+++}$ | 0.29 |
| RA | 3D | −3.56 | mL | 9.00 | −6.71 | −0.40*** | 0.5740 | 12.10% | 0.00$^{+++}$ | 0.88 |

Data are presented as the mean difference from cardiac magnetic resonance imaging (CMR) (modality—CMR).
***$p > 0.05$.
$^{+++}$ No significant correlation with CMR.
3D, three-dimensional; AP, apical four-chamber; CT, computed tomography; CV, coefficient of variation; IQR, interquartile range; L-4CH, left apical four-chamber; LA, left atrium; LVEDV, left ventricular end-diastolic volume; LV_EF, left ventricular ejection fraction; LVESV, left ventricular end-systolic volume; OVL, overlapping of the distributions; R-4CH, right parasternal four-chamber; RA, right atrium; RVEDV, right ventricular end-diastolic volume; RV_EF, right ventricular ejection fraction; RVESV, right ventricular end-systolic volume; TEE, transesophageal.

Descriptive statistics and preliminary repeated-measures analysis of variance (RMANOVA) analyses were obtained using Systat 13.1.[j] Correlations, final ANOVA and RMANOVA, coefficient of variation (CV), and the overlapping coefficient (OVL) were carried out using SAS 9.4[k]. Where possible, published (RM) ANOVA models were modified for data set—specific variable names and numbers of investigators and images. The OVL was estimated using previously published SAS code [32]. The OVL is a direct measure of the proportion (0—1) or percent (0%—100%) of overlap of two distributions and does not require that random samples come from the same distribution or have Gaussian distributions [32]. The OVL is closely related to the effect size and for normal distributions to several other measures [33]. The CV is a unitless ratio of the standard deviation to the mean, $\sigma/\mu$, which is commonly defined as the noise-to-signal ratio. Multiplying 100, the CV is then the simple proportion $n/100$. The trend in $n$ (CV) with sample size for assessing optimal repetitions was determined by logistic regression. Repeatability was defined as the average CV for all investigators for 2D and 3D TEE parameters. Intrarater CV was determined from one randomly selected investigator, and interrater CV was determined by using the first

[j] Systat Inc., San Jose, CA, USA.
[k] SAS Institute Inc., Cary, NC, USA.

**Table 3** Repeatability, intrarater and interrater variability of two-dimensional and three-dimensional transthoracic echocardiographic indices of left ventricular and left atrial size.

| Parameter | Repeatability | Interrater CV | Intrarater CV |
|---|---|---|---|
| EDV_2D L-4CH | 15.1% | 15.1% | 15.1% |
| ESV_2D L-4CH | 27.9% | 31.0% | 28.0% |
| Grand Ave_2D L4CH | 21.5% | 23.0% | 21.6% |
| EDV_3D L-4CH | 18.9% | 16.8% | 13.8% |
| ESV_3D L-4CH | 23.2% | 21.9% | 23.3% |
| Grand Ave_3D L4CH | 21.1% | 19.4% | 18.6% |
| LVIDD_MMODE | 5.6% | 7.3% | 5.6% |
| LVIDS_MMODE | 11.9% | 12.5% | 11.9% |
| Grand Ave_MMODE | 8.8% | 9.9% | 8.8% |
| LAAO_2D | 9.0% | 10.6% | 9.0% |
| LA_3D | 15.1% | 21.2% | 15.1% |

Data are displayed as the average coefficient of variation.
2D, two-dimensional; 3D, three-dimensional; coefficient of variation, CV; EDV, end-diastolic volume; ESV, end-systolic volume; grand ave = (CV diastole + CV systole)/2; L-4CH, left apical four-chamber; LA, left atrium; LAAO, left atrium to aorta ratio; LVIDD, left ventricular internal diastolic dimension; LVIDS, left ventricular internal systolic dimension; MMODE, motion mode echocardiography.

**Table 4** Repeatability of parameter measurement.

| Parameter | CV | LL | UL |
|---|---|---|---|
| LV_2D L-4CH | 8.9% | 7.0% | 12.5% |
| LV_3D L-4CH | 8.6% | 6.7% | 12.0% |
| LV_MMODE | 4.3% | 3.4% | 5.9% |
| LAAO_2D | 9.5% | 7.4% | 13.3% |
| LA_3D | 12.0% | 9.6 | 16.8% |

Data are displayed as the grand average coefficient of variation for n = 25.
CV, coefficient of variation; grand ave = (CV diastole + CV systole)/2; L-4CH, left apical four-chamber; LA_3D, left atrial volume three-dimensional; LAAO_2D, left-atrial-to-aorta ratio; LL, lower limit; LV_2D, left ventricular volume two-dimensional, LV_3D, left ventricular volume three-dimensional; LV_MMODE, left ventricular dimension motion mode echocardiography; UL, upper limit.

study day of all dogs from each of the investigators.

## Results

All dogs were safely anesthetized with no adverse events. The mean anesthesia time was 205 min (±standard deviation 48). Parameters and results for all dogs are summarized in Table 1.

### Left ventricular volume

Mean differences, 95% confidence interval (CI), and OVL between each modality and CMR were not statistically significant different. Specifically, 3D TTE systolic and diastolic dimensions had the lowest average CV (6.45%), highest average OVL (>80%), and correlated in both systole and diastole with CMR. Diastolic and systolic CTA means were closest to CMR with the smallest interquartile range; however, only systolic dimensions were correlated ($r_s = 0.55$, $p = 0.02$). All modalities had acceptable average CV of <15% (Table 2).

### Left ventricular EF

Computed tomography angiography and 2D TEE had high OVL (>86%) and mean differences close to zero; however, only CTA was correlated ($r_s = 0.61$, $p = 0.01$) with CMR. Ejection fraction was underestimated by all modalities except 2D TEE. Only 3D TTE had a notably small (−4.30%) ($p = 0.025$) mean difference for EF but was correlated with CMR ($r_s = 0.67$, $p = 0.001$).

### LA size

Mean difference in LA volume, OVL, CV, and correlation was similar for 2D TTE and 3D TTE. Overall, CTA was closest to CMR with high OVL (90%) but did not correlate ($p = 0.68$).

### Right ventricular volume

All modalities underestimated RV EDV and ESV. All 2D TTE estimates of mean RV volume in systole and diastole were significantly different than CMR, with low OVL, high CV, and no correlation. For 3D TTE, mean difference of RV ESV was insignificant; however, mean difference of RV EDV was significant ($p = 0.001$). Three-dimensional TTE had moderate OVL (58–65%) and correlated with CMR ($r_s = 0.66$–$0.86$, $p = 0.002$). The CV for 3D TTE estimates of RV EDV and ESV were 11.4% and 15.1%, respectively.

### Right ventricular EF

The 2D TTE estimates of RV EF from the L-4CH had a mean difference closest to zero and the CI contained zero. This view had moderate OVL (66%) but did not correlate with CMR ($p = 0.57$). The CV for RV EF was >21% for all modalities.

**Table 5** Summary of clinical questions, data collected, and primary statistical analyses performed.

| Data set | Question | Primary analyses | Result |
|---|---|---|---|
| (a) A single observer measured heart chambers and function in six dogs using multiple modalities under one anesthetic event (2D TTE, 3D TTE, 2D TEE, CTA, CMR) | (1) Agreement between CMR and other modalities | Spearman and Pearson correlations<br>Repeated measures analysis of variance | All data in Tables 1 and 2 |
| | (2) Repeatability (within each modality) | CV<br>Bland Altman, OVL, descriptive statistics (mean difference from CMR, interquartile range, 95% confidence intervals) | |
| (b) Four observers obtained their own images and made their own measurements of the LV and LA in five dogs. Each dog was imaged in 5 separate sessions over 3 days | (2) Repeatability (within an observer and modality)<br>(3) Repeatability (between observers within a modality) | CV by modality, dog, replicate | All data in Table 3 |
| (c) A single observer obtained images on one dog in five separate sessions over 3 days and three different observers measured the same images. | (3) Repeatability (within an observer and between observers measuring the same images) | CV by modality, dog, replicate | All data in Table 4 |
| | (4) Optimal number of repetitions required to establish a representative mean | Logistic regression of sample size against the lower and upper limits of CV | |

CMR, cardiac magnetic resonance imaging; CTA, computed tomography angiography; CV, coefficient of variation; LA, left atrium; LV, left ventricle; OVL, overlapping of the distributions; 2D TEE, transesophageal two-dimensional echocardiography; 2D TTE, transthoracic two-dimensional echocardiography; 3D TTE, transthoracic three-dimensional echocardiography.

### Right atrial volume

Two-dimensional TTE and 3D TTE underestimated mean RA volume in comparison to CMR. Mean differences for RA volume was closest to zero (−3.56 mL) for 3D TTE with moderate OVL (57%) but did not correlate with CMR ($p = 0.88$).

### Automated border detection software 3D TTE

In our study, we deliberately avoided heavy-handed measurement adjustments whenever an automated option was available. In instances of egregious border error (LV-2%, RV-8%, LA-30%, RA-30%), manual corrections were required.

### TTE repeatability

Average CV for repeatability and intrarater and interrater measurements of variability for selected LA and LV parameters are summarized in Table 3, while Table 4 represents the CV of measuring the same images by 3 investigators. Evaluation of LV size via M-mode had the highest average repeatability (CV = 8.8%) and lowest average intrarater and interrater variability for both image acquisition (CV = 9.3%) and measurement (CV = 4.3%). Average repeatability of 3D TTE image acquisition (CV = 21.1%) and measurement (CV = 8.6%) was similar to 2D TTE image acquisition (CV = 21.5%) and measurement (CV = 8.9%). Average intrarater and interrater variability of 3D TTE (CV = 18.9%) was also similar to 2D TTE (CV = 22.3%). Assessment of LA:Ao via 2D TTE had better repeatability for image acquisition (CV = 9.0%) and measurement (CV = 9.5%) than 3D TTE volume acquisition (CV = 15.1%) and measurement (CV = 12.0%). M-mode assessment of LV size in diastole and systole achieved acceptable precision after five repeated measurements, while 3D TTE and 2D TTE required 10 and 15 repetitions, respectively.

## Discussion

This study is the first direct comparison of 2D TTE, 3D TTE, 2D TEE, and CTA, with CMR for assessment

of cardiac size and function in dogs. Quantification of cardiac size and function in dogs is most commonly performed using 2D TTE alone or in combination with M-mode and are dependent on operator technique, acoustic windows, and geometric assumptions regarding heart shape. Volumetric methods using 3D TTE, CTA, and CMR in humans patients have demonstrated substantial improvements over conventional 2D TTE [5,34,35]. Our study applied multiple statistical methods to reach conclusions regarding which modalities best agree with the reference standard, CMR.

We have reported mean differences and CI between modalities and CMR. However, because the fractile of a mean varies with the shape of distribution and sample size, a statistically significant difference does not imply anything about the clinical relevance of the difference between the modality and CMR. For example, when the significantly standardized difference ($d$) is 0.5 (Cohen's 'medium'), the OVL of the distributions for a modality and CMR is 0.8 (80%), and when $d = 0.8$ (Cohen's 'large') the OVL is 0.69 (69%). To retain qualitative and quantitative meanings of CMR measurements, an alternative modality must have both a correlation with and OVL distribution similar to CMR. The significance of a difference between means may or may not be clinically relevant when these requirements are met.

Against the CMR reference standard, 3D TTE was superior to other modalities for assessing LV dimensions (EDV, ESV): it was reproducible (CV = 6.2—6.7%), was correlated ($r_s = 0.61—0.63$), and had high OVLs (81.5—82.7%) with CMR. The CV and OVL were considered acceptable for CTA, 2D TTE, and 2D TEE; however, these modalities often did not correlate with and had large variances compared to CMR. Differences between mean LV volumes calculated by 2D TEE and CMR were small; however, not all parameters (EF, LVESV) correlated. As reported in Table 1, when specifically evaluating LV volume, most dogs in this study had an LV size of 50 mL in diastole and 22 mL in systole. All modalities were within ±3 mL (6%) of CMR. In systole, all modalities had a mean difference from CMR ±1 mL (4.5%). These differences are acceptable for clinical agreement. Thus, global LV size and function in normal dogs can be determined using all modalities, although 3D TTE had the best overall agreement with CMR.

Quantitative assessment of LA size is important for risk stratification and prognosis of many cardiovascular diseases [36,37]. The LA:Ao is a commonly used method for detecting LA enlargement in veterinary practice [27,36]. Quantification of LA volume may, therefore, be clinically useful especially if the interrater and intrarater CV are acceptable or better than LA:Ao, regardless of correlation with CMR. This study found that, compared with CMR, CTA estimation of LA volume was superior to 2D TTE (10% overestimation) and 3D TTE (10% underestimation). Using CTA, LA volume was overestimated by a clinically acceptable value of 3.5%, in comparison to CMR, but no modalities correlated with CMR.

Evaluation of the RV is challenging because of complex anatomy and mechanics. The cornerstone of RV assessment is 2D TTE; however, numerous limitations exist, and it has weak correlation to CMR [38]. Two-dimensional TTE overlooks RV segments, such as the RV outflow tract, whereas 3D TTE and other modalities more accurately estimate RV volume [5]. In our study, RV size was systematically underestimated by 2D TTE (by 55%) and 3D TTE (by 28%) in comparison to CMR. Importantly, 3D TTE correlated in diastole ($r_s = 0.86$) and systole ($r_s = 0.66$) to CMR with moderate OVL (58 and 65%). Thus, 3D TTE provides clinically useful estimates of RV volume compared with CMR. However, 2D TTE and 3D TTE RV EF did not correlate. As such, RV function remains a subjective assessment in most cases.

Right atrial size was underestimated by 2D TTE (36%) and 3D TTE (16%) and did not correlate with CMR. These findings agree with previously reported differences in human studies [39].

The most commonly used method for assessing LV size, M-mode, had the highest overall repeatability and lowest intrarater and interrater variability (<10%). This result is expected given the ubiquity of this imaging modality as part of everyday clinical practice for cardiologists. Volumetric assessment of the LV is not routinely performed on every patient at our institution, and therefore, an increase in the CV was expected. This study shows that despite its novelty, 3D TTE had similar repeatability and intrarater and interrater CV to 2D TTE. Using 3D TTE, four orthogonal images are obtained simultaneously, and volumetric assessment is performed via automated software. This decreases the level of observer subjectivity and may explain why 3D TTE had a lower CV than 2D TTE. In addition, because 2D TTE volumes were derived from monoplane SMOD, variations in image acquisition results in larger differences via greater geometric assumptions. Undoubtedly, newer generations of 3D and specifically border detection software for both 2D TTE and 3D TTE as well as newer generation 2D and 3D transducers will further improve accuracy and interrater and intra-rater variability, which may be particularly relevant in small patients. Updates to

both software and transducers have already occurred since this study was completed. The authors have used these upgrades and subjectively think improvements in image quality, frame rates, and automated border detection are superior. Even if the exact interrater and intrarater CV reported herein cannot be expected in every center, the relative magnitudes provide readers with approximate expectations.

Finally, we sought to determine the CV for image measurements. Given the novelty of 3D TTE, comparison with standard 2D TTE image measurements was important. Three investigators measured images acquired by a fourth observer (M-mode, 2D TTE, and 3D TTE). Average CV for measuring the LV with M-mode was 4.3%, and although the CV was twice this for 3D TTE (8.6%) and 2D TTE (8.9%), both are considered acceptable. Measurements of LA:Ao had lower CV (9.5%) than 3D TTE LA volumes (12.0%). Subjectively, automated border detection software often had difficulty identifying the LA endocardium, partially explaining this finding, while LA:Ao measurements are performed routinely making this measurement common for all investigators.

Commonly, scanners acquire and measure 3—5 images to determine a mean. In this study, 5 stored images of each parameter were measured by each of 3 investigators, and this was repeated 5 times for a total of 25 values per parameter per investigator. We sought to determine the optimum number of repetitions required to ensure a representative value. Logistic regression indicated that the upper bound of the CV increases as the number of measurements decreases. While the average was minimally changed, the range between lower and upper bounds increased, and therefore, a single measurement became an increasingly inaccurate estimate of the mean. In our study, M-mode assessment of LV size achieved acceptable precision (CV $\leq$ 15%) after 5 repetitions, while 3D TTE and 2D TTE required 10 and 15 repetitions, respectively. We defined acceptable precision based on other previously proposed limits of CV [40—42]. Particularly, when comparing 3D TTE and 2D TTE, this study highlights how small improvements in repeatability can substantially impact repetition requirements. These data may be useful in study design protocols planning to use echocardiographic assessment as an outcome variable.

Limitations of this study include lack of contrast in RV and RA for CTA images, making assessment of RV and RA impossible with this modality. For comparison between different modalities, all dogs were placed under general anesthesia. Imaging could not be performed simultaneously, and the order of imaging was not randomized. Therefore, despite all attempts to maintain a consistent hemodynamic steady state, time under anesthesia could affect agreement between modalities. The CV within a modality is not likely increased by the use of general anesthesia as image acquisition was performed over a short period of time with little change in any hemodynamic parameters; however, because these patients were immobile, ventilated, and had slow regular heart rates, the CV may have been improved, and these values should not be expected in awake patients. Patients were mechanically ventilated in our study during imaging of all modalities. With respect to RV volume and function, CMR and CTA images were acquired during end-expiration, while echocardiographic images were obtained in early-inspiration and throughout expiration. While peak-inspiration was avoided, respiratory variation can affect right heart size and function, and this may have further contributed to the discrepancy between echocardiography and CMR parameters. In addition, our results are dependent on the technology of the automated border detection software. Since the time of completing this study, software, especially as it relates to automated border detection in 2D TTE, has substantially improved, and the 3D TTE probe has improved to 4V technology. The 2D image quality and frame rate of 3D TTE probes are vital to accuracy and have improved appreciably with the 4V probe. Therefore, our results must be interpreted in light of the technology we used. Finally, we used CMR as the reference standard, and conclusions could change using a different modality as the reference. In addition, when assessing blood pool volumes of the LV and RV via CMR, papillary muscles and large trabeculations were excluded, while they were included for echocardiography. These are considered standard measurement techniques for these modalities, and it is unlikely to significantly change CMR-derived measurements [43]. As dogs in this study were healthy, and moderately large, it should not be assumed that the relationships among these modalities are the same for dogs with cardiac disease or small patients.

## Conclusions

This study found that LV size, RV size, RV EF, and RA size from 3D TTE compared best with CMR. Of the modalities examined, 3D TTE was typically the most reproducible and had lower intrarater and interrater variability than 2D TTE. The CTA estimates of LV EF and LA size compared most favorably with CMR.

## Conflicts of Interest Statement

The authors do not have any conflicts of interest to disclose.

## Acknowledgments

The authors thank Mark Lennox and Christine Pelham for the technical assistance and expertise with CMR and CTA imaging.

## References

[1] Thomas WP, Gaber CE, Jacobs GJ, Kaplan PM, Lombard CW, Moise NS, Moses BL. Recommendations for standards in transthoracic two-dimensional echocardiography in the dog and cat. echocardiography committee of the specialty of cardiology, American College of veterinary internal medicine. J Vet Intern Med 1993;7:247—52.

[2] Kienle RD, Thomas WP, Rishniw M. Biplane transesophageal echocardiography in the normal cat. Vet Radiol Ultrasound 1997;38:288—98.

[3] Chukwu EO, Barasch E, Mihalatos DG, Katz A, Lachmann J, Han J, Reichek N, Gopal AS. Relative importance of errors in left ventricular quantitation by two-dimensional echocardiography: insights from three-dimensional echocardiography and cardiac magnetic resonance imaging. J Am Soc Echocardiogr 2008;21:990—7.

[4] Constantine G, Shan K, Flamm SD, Sivananthan MU. Role of MRI in clinical cardiology. Lancet 2004;363:2162—71.

[5] Sugeng L, Mor-Avi V, Weinert L, Niel J, Ebner C, Steringer-Mascherbauer R, Schmidt F, Galuschky C, Schummers G, Lang RM, Nesser H. Quantitative assessment of left ventricular size and function: side-by-side comparison of real-time three-dimensional echocardiography and computed tomography with magnetic resonance reference. Circulation 2006;114:654—61.

[6] Caputo GR, Tscholakoff D, Sechtem U, Higgins CB. Measurement of canine left ventricular mass by using MR imaging. AJR Am J Roentgenol 1987;148:33—8.

[7] Markiewicz W, Sechtem U, Kirby R, Derugin N, Caputo GC, Higgins CB. Measurement of ventricular volumes in the dog by nuclear magnetic resonance imaging. J Am Coll Cardiol 1987;10:170—7.

[8] Mor-Avi V, Sugeng L, Weinert L, MacEneaney P, Caiani EG, Koch R, Salgo IS, Lang RM. Fast measurement of left ventricular mass with real-time three-dimensional echocardiography: comparison with magnetic resonance imaging. Circulation 2004;110:1814—8.

[9] Keller AM, Gopal AS, King DL. Left and right atrial volume by freehand three-dimensional echocardiography: in vivo validation using magnetic resonance imaging. Eur J Echocardiogr 2000;1:55—65.

[10] Rodevan O, Bjornerheim R, Ljosland M, Maehle J, Smith HJ, Ihlen H. Left atrial volumes assessed by three- and two-dimensional echocardiography compared to MRI estimates. Int J Card Imag 1999;15:397—410.

[11] LeBlanc N, Scollan K, Sisson D. Quantitative evaluation of left atrial volume and function by one-dimensional, two-dimensional, and three-dimensional echocardiography in a population of normal dogs. J Vet Cardiol 2016;18:336—49.

[12] LeBlanc NL, Scollan KF, Stieger-Vanegas SM. Cardiac output measured by use of electrocardiogram-gated 64-slice multidector computed tomography, echocardiography, and thermodilution in healthy dogs. Am J Vet Res 2017;78:818—27.

[13] Sieslack AK, Dziallas P, Nolte I, Wefstaedt P, Hungerbühler SO. Quantification of right ventricular volume in dogs: a comparative study between three-dimensional echocardiography and computed tomography with the reference method magnetic resonance imaging. BMC Vet Res 2014;10:242.

[14] Qin JX, Jones M, Travaglini A, Song J-M, Li J, White RD, Tsujino H, Greenberg NL, Zetts AD, Panza JA, Thomas JD, Shiota T. The accuracy of left ventricular mass determined by real-time three-dimensional echocardiography in chronic animal and clinical studies: a comparison with postmortem examination and magnetic resonance imaging. J Am Soc Echocardiogr 2005;18:1037—43.

[15] Sapin PM, Gopal AS, Clarke GB, Smith MD, King DL. Three-dimensional echocardiography compared to two-dimensional echocardiography for measurement of left ventricular mass anatomic validation in an open chest canine model. Am J Hypertens 1996;9:467—74.

[16] Anwar AM, Soliman OII, ten Cate FJ, Nemes A, McGhie JS, Krenning BJ, van Geuns RJ, Galema TW, Geleijnse ML. True mitral annulus diameter is underestimated by two-dimensional echocardiography as evidenced by real-time three-dimensional echocardiography and magnetic resonance imaging. Int J Cardiovasc Imag 2007;23:541—7.

[17] Leibundgut G, Rohner A, Grize L, Bernheim A, Kessel-Schaefer A, Bremerich J, Zellweger M, Buser P, Handke M. Dynamic assessment of right ventricular volumes and function by real-time three-dimensional echocardiography: a comparison study with magnetic resonance imaging in 100 adult patients. J Am Soc Echocardiogr 2010;23:116—26.

[18] Badano LP, Agricola E, Perez de Isla L, Gianfagna P, Zamorano JL. Evaluation of the tricuspid valve morphology and function by transthoracic real-time three-dimensional echocardiography. Eur J Echocardiogr 2009;10:477—84.

[19] Jurcut R, Giusca S, La Gerche A, Vasile S, Ginghina C, Voigt J-U. The echocardiographic assessment of the right ventricle: what to do in 2010? Eur J Echocardiogr 2010;11:81—96.

[20] Singh RM, Singh BM, Mehta JL. Role of cardiac CTA in estimating left ventricular volumes and ejection fraction. World J Radiol 2014;6:669—76.

[21] Lee D, Li D, Jug B, Papazian J, Budoff M. Diagnostic accuracy of 64 slice multidetector coronary computed tomographic angiography in left ventricular systolic dysfunction. Int J Cardiol Heart Vasc 2015;8:42—6.

[22] Scali MC, Basso M, Gandolfo A, Bombardini T, Bellotti P, Sicari R. Real time 3D echocardiography (RT3D) for assessment of ventricular and vascular function in hypertensive and heart failure patients. Cardiovasc Ultrasound 2012;10:27.

[23] Nabity MB, Boggess MM, Kashtan CE, Lees GE. Day-to-day variation of the urine protein: creatinine ratio in female dogs with stable glomerular proteinuria caused by X-linked hereditary nephropathy. J Vet Intern Med 2007;21:425—30.

[24] Lees GE, Helman RG, Kashtan CE, Michael AF, Homco LD, Millichamp NJ, Camacho ZT, Templeton JW, Ninomiya Y, Sado Y, Naito I, Kim Y. New form of X-linked dominant hereditary nephritis in dogs. Am J Vet Res 1999;60:373—83.

[25] Lees GE, Kashtan CE, Michael AF, Helman RG, Naito I, Ninomiya Y, Sado Y, Kim Y. Expression of the alpha6 chain of type IV collagen in glomerular basement membranes of healthy adult dogs. Am J Vet Res 2000;61:38—41.

[26] Bell RJ, Lees GE, Murphy KE. X chromosome inactivation patterns in normal and X-linked hereditary nephropathy Carrier dogs. Cytogenet Genome Res 2008;122:37—40.
[27] Rishniw M, Erb HN. Evaluation of four 2-dimensional echocardiographic methods of assessing left atrial size in dogs. J Vet Intern Med 2000;14:429—35.
[28] Wess G, Sarkar R, Hartmann K. Assessment of left ventricular systolic function by strain imaging echocardiography in various stages of feline hypertrophic cardiomyopathy. J Vet Intern Med 2010;24:1375—82.
[29] Visser LC, Scansen BA, Schober KE, Bonagura JD. Echocardiographic assessment of right ventricular systolic function in conscious healthy dogs: repeatability and reference intervals. J Vet Cardiol 2015;17:83—96.
[30] Rudski LG, Lai WW, Afilalo J, Hua L, Handschumacher MD, Chandrasekaran K, Solomon SD, Louie EK, Schiller NB. Guidelines for the echocardiographic assessment of the right heart in adults: a report from the American society of echocardiography endorsed by the European association of echocardiography, a registered branch of the European society of cardiology, and the Canadian society of echocardiography. J Am Soc Echocardiogr 2010;23:685—713. quiz 786—8.
[31] Muraru D, Badano LP, Piccoli G, Gianfagna P, Del Mestre L, Ermacora D, Proclemer A. Validation of a novel automated border-detection algorithm for rapid and accurate quantitation of left ventricular volumes based on three-dimensional echocardiography. Eur J Echocardiogr 2010; 11:359—68.
[32] Martens E, Pestman W, Boer A, Belitser V, Klungel OH. The use of the overlapping coefficient in propensity score analysis. Pharmacoepidemiol Drug Saf 2007;16.
[33] Royston P, Altman DG. Visualizing and assessing discrimination in the logistic regression model. Stat Med 2010;29: 2508—20.
[34] Serres F, Chetboul V, Tissier R, Poujol L, Gouni V, Carlos Sampedrano C, Pouchelon JL. Comparison of 3 ultrasound methods for quantifying left ventricular systolic function: correlation with disease severity and prognostic value in dogs with mitral valve disease. J Vet Intern Med 2008;22: 566—77.
[35] Takuma S, Ota T, Muro T, Hozumi T, Sciacca R, Di Tullio MR, Blood DK, Yoshikawa J, Homma S. Assessment of left ventricular function by real-time 3-dimensional echocardiography compared with conventional non-invasive methods. J Am Soc Echocardiogr 2001;14:275—84.
[36] Hansson K, Häggström J, Kvart C, Lord P. Left atrial to aortic root indices using two-dimensional and M-mode echocardiography in cavalier King Charles spaniels with and without left atrial enlargement. Vet Radiol Ultrasound 2002;43:568—75.
[37] Borgarelli M, Savarino P, Crosara S, Santilli RA, Chiavegato D, Poggi M, Bellino C, La Rosa G, Zanatta R, Haggstrom J, Tarducci A. Survival characteristics and prognostic variables of dogs with mitral regurgitation attributable to myxomatous valve disease. J Vet Intern Med 2008;22:120—8.
[38] Surkova E, Muraru D, Iliceto S, Badano LP. The use of multimodality cardiovascular imaging to assess right ventricular size and function. Int J Cardiol 2016;214:54—69.
[39] Whitlock M, Garg A, Gelow J, Jacobson T, Broberg C. Comparison of left and right atrial volume by echocardiography versus cardiac magnetic resonance imaging using the area-length method. Am J Cardiol 2010;106: 1345—50.
[40] Margiocco ML, Bulmer BJ, Sisson DD. Doppler-derived deformation imaging in unsedated healthy adult dogs. J Vet Cardiol 2009;11:89—102.
[41] Simpson KE, Craig Devine B, Gunn-Moore DA, French AT, Dukes-McEwan J, Koffas H, Moran CM, Corcoran BM. Assessment of the repeatability of feline echocardiography using conventional echocardiography and spectral pulse-wave Doppler tissue imaging techniques. Vet Radiol Ultrasound 2007;48:58—68.
[42] Chetboul V, Athanassiadis N, Concordet D, Nicolle A, Tessier D, Castagnet M, Pouchelon JL, Lefebvre HP. Observer-dependent variability of quantitative clinical endpoints: the example of canine echocardiography. J Vet Pharmacol Therapeut 2004;27:49—56.
[43] Sievers B, Kirchberg S, Bakan A, Franken U, Trappe H-J. Impact of papillary muscles in ventricular volume and ejection fraction assessment by cardiovascular magnetic resonance. J Cardiovasc Magn Reson 2004;6:9—16.